Audio Engineering Society

Convention Paper 6881

Presented at the 121st Convention
2006 October 5–8 San Francisco, CA, USA

High-Accuracy Full-Sphere Electro Acoustic Polar Measurements at High Frequencies using the HELS Method

Huancai Lu [1], Sean Wu [2], and D. B. (Don) Keele, Jr.[3]

[1] SenSound LLC, Grosse Pointe Farms, MI, 48236, USA
huancai.lu@sensound.com

[2] SenSound LLC, Grosse Pointe Farms, MI, 48236, USA
sean.wu@sensound.com

[3] Harman International Industries, Northridge, CA, 91329, USA
DKeele@harman.com

ABSTRACT

Traditionally, high-accuracy full-sphere polar measurements require dense sampling of the sound field at very-fine angular increments, particularly at high frequencies. The proposed HELS (Helmholtz Equation Least Squares) method allows this restriction to be relaxed significantly. Using this method, far fewer sampling points are needed for full and accurate reconstruction of the radiated sound field. Depending on the required accuracy, sound fields can be reconstructed using only 10 to 20% of the number of sampling points required by conventional techniques. The HELS method allows accurate reconstruction even for sample spacing that violates the Nyquist spatial sampling rate in certain directions. This paper examines the convergence of HELS solutions via theory and simulation for reconstruction of the acoustic radiation patterns generated by a rectangular plate mounted on an infinite rigid flat baffle. In particular, the impact of the numbers of expansion terms and measurement points as well as errors imbedded in the input data on the resultant accuracy of reconstruction is analyzed.

1. INTRODUCTION

Loudspeakers are often designed based on their predicted and measured acoustical performances, one of them being the radiation pattern. Accurate prediction of a radiation pattern requires the knowledge of source characteristics, boundary conditions, etc., which is usually very difficult. So in practice, the radiation patterns are measured instead. These measurements are taking place in the far field as defined by AES Standards [1, 2, 3, 4]. To ensure high accuracy and spatial resolution, AES also requires that measurements be taken at an angular resolution equal to or less than 1°. This super fine angular resolution coupled with a far-field measurement requirement result in an excessive number of measurements. For example, at 1-meter distance and with a 1° angular resolution one would need to take 64,800 measurement points over entire 180° polar angle and 360° azimuthal angle ranges, which is unrealistic in practice by any means. The spacing between two neighboring measurement microphones at 1-meter distance is Δs = 1.7cm, which means that even if we use the minimum Nyquist spatial sampling rate of 2.5 measurement points per wavelength, we can only depict radiation pattern up to $f=C/\lambda=$ 340/(2.5×0.017)=8000 Hz. It has been found [1] that when coarse angular resolution is adopted, for example, at 2°, 5°, and 10°, nulls and lobes in a radiation pattern may be lost and its image be distorted. This example shows how difficult it is to obtain an accurate radiation pattern at high frequencies. So there is a great demand in the speaker industry to search for alternatives that can offer accurate descriptions of speaker radiation patterns with much fewer measurement points.

In this paper, we present a methodology based on expansion theory, which has been used in near-field acoustical holography known as the HELS (Helmholtz Equation Least Squares) method [5, 6]. Specifically, HELS expresses the acoustic pressure through an expansion of the spherical wave functions and the expansion coefficients are determined by matching the assumed-form solution to the measured data. Note that if measurement points are placed on a spherical surface enclosing the source, the HELS solutions will be exact. Moreover, the number of expansion terms required in HELS is correlated to the dimension of the source and frequency of interest. This gives HELS an advantage in dealing with small sources. For example, consider a speaker with a characteristic dimension a = 0.16m at the same frequency as that considered above: 8000Hz so a dimensionless frequency is $ka = (2\pi f a) / c = 2\pi\times8000\times0.16/340 \approx 23$. Previous studies have shown that for a given ka, it is enough to expand the spherical wave functions up to $n = ka$ in an expansion [7]. Therefore, the number of expansion terms is $J = (n + 1)^2$. This means that we need $M \geq J = (ka + 1)^2 =$ 596 measurement points only, which is less than 1% of those required by AES Standards. Note that the formula for estimating the numbers of expansion terms and measurement points have nothing to do with the Nyquist spatial sampling rate. Therefore, with HELS we may be able to cut down the number of measurement points significantly.

2. HELMHOLTZ EQUATION LEAST SQUARES (HELS) METHOD

HELS has been shown to be an effective nearfield acoustical holography (NAH) methodology to reconstruct the entire acoustic field generated by an arbitrary source in 3D space, including a 3D source surface [5, 6]. In this method, the acoustic pressure is expressed in terms of a superposition of spherical wave functions that consist of the spherical Hankel functions and spherical harmonics.

$$p(\mathbf{x};\omega) = \sum_{j=1}^{J} \Psi_j^{(1)}(\mathbf{x};\omega) C_j(\omega) \qquad (1)$$

where $\Psi_j^{(1)}$ is the j^{th} particular solution to the Helmholtz equation in any coordinate system. For example, using the spherical coordinates we can write $\Psi_j^{(1)}$ as

$$\Psi_j^{(1)} \equiv \Psi_{nl}^{(1)}(r,\theta,\phi;\omega) = h_n^{(1)}(kr) Y_n^l(\theta,\phi) \qquad (2)$$

where $h_n^{(1)}(kr)$ indicates the spherical Hankel functions of order n of the first kind, k is the acoustic wavenumber, $Y_n^l(\theta,\phi)$ are the spherical harmonics, and the indices j, n, and l in Eq. (2) are related via $j = n^2 + n + l + 1$ with n starting from 0 to K and l varying from $-n$ to n. Hence, for each n and l we have $j = 1$ to J, where $J = (K + 1)^2$ represents the maximum number of expansion functions.

The expansion coefficients C_j are determined by matching the assumed-form solution Eq. (1) to the acoustic pressure $\tilde{p}(\mathbf{x}_m^{\Gamma};\omega)$ measured on a conformal surface Γ around the source,

$$p_J(\mathbf{x}_m^{\Gamma};\omega) = \tilde{p}(\mathbf{x}_m^{\Gamma};\omega) \qquad (3)$$

where $\mathbf{x}_m^{\Gamma} \in \Gamma$, $m = 1$ to M $(M > J)$, M is the measurement points.

Normally, we take more measurement points than the number of expansion functions to form an over-determined system and use least squares to minimize the errors in calculating the expansion coefficients.

$$\min_{C_1,C_2,\cdots,C_J} \left\| p_J(\mathbf{x}_m^{\Gamma};\omega) - \tilde{p}(\mathbf{x}_m^{\Gamma};\omega) \right\|_2^2 \qquad (4)$$

Once the coefficients C_j are specified, the acoustic pressure can be reconstructed using Eq. (1).

It is emphasized that Eq. (1) is valid in an exterior region including an arbitrarily shaped source surface S. The completeness of an expansion in terms of the particular solutions to Helmholtz equation was first demonstrated by Vekua [8]. Isakov and Wu [9] gave rigorous mathematical justifications of using Eq. (1), least squares, and quasi-solution methods to reconstruct acoustic radiation from an arbitrary source. In particular, they proved that Eq. (1) outside a sufficiently smooth, convex, and bounded domain can be approximated by a family of special solutions [9]. By using Eq. (1) and the conditional stability estimates in the Cauchy problem for an elliptic equation, Isakov and Wu showed that these special solutions are bounded on and outside a source surface and converge to the exact solution, provided that they converge on a measurement surface. The same conclusions hold for reconstructing the acoustic field in an interior region as well [9].

In this paper, we use HELS method to reconstruct radiation patterns from a highly non-spherical source. The input data are

collected on a spherical surface in the far field of the target source. The number of input data is much smaller than what is required by AES Standards. If these input data are used to depict radiation patterns directly, they will be distorted because many side nulls and lobes are missing, especially at high frequencies.

The main objective of this paper is to examine the feasibility of using HELS method to produce a correct radiation pattern based on a relatively small number of measurement points. Note that such a problem can be considered a mildly ill-posed problem since one attempts to fill gaps among measurement microphones with the acoustic pressures based on a finite number of data points measured on the same surface. This problem is ill-posed because the input data are apparently incomplete. This is especially true at high frequencies where there are many side lobes and nulls. On the other hand, the ill-posedness difficulty is not as sever as a typical NAH application because the reconstructed acoustic pressures are on the same surface as the measurement surface. Nevertheless, we need to regularize the transfer matrix to ensure a satisfactory reconstruction.

Another objective of this paper is to examine the suitability and robustness of HELS method to reconstruct the acoustic field generated by arbitrary source geometry at high frequencies. While HELS can produce an exact solution outside the minimum sphere that circumscribes the source for an exterior problem or inside the maximum sphere that inscribes the source for an interior problem, the number of expansion terms and that of measurement points necessary to reconstruct the details of an acoustic field are not clear. In other words, what is the minimum number of the expansion terms in HELS needed to describe all side lobes and nulls in reconstruction? What is the minimum number of measurement points required to avoid spatial aliasing in reconstruction? Most importantly, how robust is HELS method? This is critical because in practice all measured data contain errors to certain degree. How sensitive are the HELS formulations to errors in the input data? Will the errors imbedded in the input data be amplified in the reconstruction process?

These questions are addressed in this paper. Without a loss of generality, we select a source to be a rectangular plate mounted on an infinite, rigid baffle. The reason for selecting this test object is that a rectangular plate represents a class of geometries that cannot be exactly described by the spherical Hankel functions and spherical harmonics, which are embedded in the HELS formulations. On the other hand, analytic solution is readily available so that the accuracy in reconstruction can be studied in detail.

3. RADIATION PATTERNS OF A BAFFLED RECTANGULAR PLATE

The formulation for predicting the radiation pattern of a rectangular plate mounted on an infinite, rigid baffle is well know [10], whose standard normalized pressure amplitude is given by

$$P_n(\phi_1,\phi_2)=\frac{\sin\left(\frac{\pi d_1 \sin\phi_1}{\lambda}\right)}{\frac{\pi d_1 \sin\phi_1}{\lambda}}\frac{\sin\left(\frac{\pi d_2 \sin\phi_2}{\lambda}\right)}{\frac{\pi d_2 \sin\phi_2}{\lambda}} \tag{5}$$

where ϕ_1 and ϕ_2 represent the angular variables along the longitudinal and transverse directions, respectively, d_1 and d_2 are the length and width of the plate, respectively, and λ is the wavelength of the frequency of interest.

In this paper, Eq. (5) is used to generate the field acoustic pressure at a finite number of points on a spherical surface. These acoustic pressures are taken as input data to the HELS formulations to reconstruct the radiation patterns over a frequency range of 250 to 16000Hz. These reconstructed acoustic radiation patterns are then compared with those generated by Eq. (5).

The objectives of this numerical simulation are to see: 1) if HELS is able to recover all details in radiation patterns such as side lobes and nulls at high frequencies; 2) the impacts of measurement points and errors imbedded in input data on the accuracy and resolution of reconstruction; 3) the potential benefits of using HELS to generate radiation patterns in practice.

The test object is a flat rectangular plate of dimensions 45 × 160mm mounted on an infinite, rigid baffle. For convenience, we use the Cartesian coordinate system with its origin at the geometric center of the plate. Further, we define the *z*-axis to be in the normal direction and *x* and *y* axes to lie on the plate pointing in the transverse and longitudinal directions, respectively. The input data are collected over a hemispherical surface of a radius r = 1m with uniform angular intervals $\Delta\phi_1$ and $\Delta\phi_2$, where ϕ_1 denotes an angle between the *z*-axis and the projection of the line that links the origin of the coordinate system to observation point, and that is in the plane normal to the surface and parallel to d_2. Similarly, ϕ_2 denotes an angle between the *z*-axis and the projection of the line that links the origin of the coordinate system to an observer, and that is in the plane normal to the surface and parallel to d_1. For clarity, only one quadrant of this hemispherical surface is depicted in Figure 1.

Figure 2 shows the grid on which the input data are collected using Eq. (5). Note that the spacing among individual nodes, $\Delta\phi_1$ and $\Delta\phi_2$, are much greater than that required by the AES Standards. There are no sources other than this vibrating plate and the field is unbounded.

4. RESULTS AND DISCUSSIONS

The acoustic pressures generated on a coarse grid over a hemispherical surface of radius 1m are taken as input to reconstruct radiation patterns on the same hemispherical surface in 1/3-octave bands from 250 to 16000Hz. For brevity, we display results at the center frequencies of these 1/3-octave bands.

4.1. Can HELS Method Recover All the Details in Radiation Patterns at High Frequencies Based on a Finite Number of Measurement Points?

To address this first question, we collect M = 410 measurement points over one quadrant with an angular resolution of $\Delta\phi_1$ =2.25° and $\Delta\phi_2$ =10°, and reconstruct acoustic pressures on 460 points, N = 460, with $\Delta\phi_1$ =2° and $\Delta\phi_2$ =10°.

Figure 3 shows comparisons of the reconstructed radiation patterns (1st, 3rd, 5th, 7th and 9th rows) and theoretical ones (2nd, 4th, 6th, 8th and 10th rows) in a linear scale projected on *y*-*z* plane at the center

frequencies of 1/3-octave bands from 250 to 6278Hz. We notice that the first side lobe appears at 2490Hz, the second side lobe at 4976Hz, and more side lobes show up after 7896HZ. To get a better view of the side lobes in the radiation patterns up to 16000Hz, we show enlarged images in Figure 4. We can see that at f = 16000Hz, ka = 25, there are seven side lobes in the longitudinal direction and the shapes and sizes of these side lobes are well preserved in the reconstructed radiation patterns.

Note that the number of side lobes in the transverse direction is less than that in the longitudinal direction. This is because the width of the plate is about ¼ of its length and therefore at a given frequency, the acoustic pressure wave can fluctuate along the transverse direction about ¼ of that along the longitudinal direction. For example, at 16000Hz, there are seven side lobes seen on the y-z plane, but only one side lobe on the x-z plane. Figure 5 shows all the reconstructed radiation patterns on x-z plane. Figure 6 illustrates comparisons of reconstructed and theoretical radiation patterns in 3D view in dB scale. The reason for selecting dB scale is to emphasize the shape and size of the side lobes, which would have been much smaller than the main lobe in a linear scale. Figure 7 gives the projection of 3D radiation patterns on the y-z plane from 3951 to 16000Hz in order to provide a clearer view of comparison of reconstructed radiation patterns vs. theoretical ones. So the answer to the question on the subtitle 4.1 is a definite yes.

It is emphasized that the numbers of measurement points in ϕ_1 and ϕ_2 directions are substantially less than the AES Standard and have severely violated the Nyquist spatial sampling requirement. For example, at f = 16000Hz the wavelength is λ = 0.0215m. If we apply the minimum Nyquist spatial sampling rate of 2.5 measurements per wavelength, we need take 183 measurement points along ϕ_1 direction or with an angular increment of $\Delta\phi_1 < 0.5°$. If we apply the same rule in the ϕ_2 direction, we will end up 33489 measurement points. Even if we use the same angular increment of $\Delta\phi_2$ =10°, we will need 1647 measurement points. Thus, it is obvious that using HELS can cut down significantly the number of measurement points in reconstructing radiation patterns.

4.2. WHAT ARE THE IMPACTS OF MEASUREMENT POINTS AND ERRORS IMBEDDED IN THE INPUT DATA ON THE ACCURACY AND RESOLUTION OF RECONSTRUCTION USING HELS?

The question one may have next is how the number of measurement points affects the end result and how robust HELS is when the input data are not error free. To address these issues, we tested cases in which the relationship between the number of expansion terms in HELS formulation and a dimensionless frequency is relaxed. This in turn will reduce the number of measurement points. For example, it is well established [9] that in using the expansion of the spherical wave functions to an acoustic field, it suffices to stop at, $n = ka$, where n is the index or order of the spherical wave function. The total number of expansion terms is given by, $J = (n + 1)^2$, which is $(ka + 1)^2$ when we stop at the expansion at any given dimensionless frequency ka. This relation may still lead to an excessive number of measurement points, especially when the characteristic dimension of the source is large.

To reduce the number of measurement points, we attempt to relax this requirement by carrying out a systematic investigation in which the measurement points M is decreased gradually, while the rest parameters remain unchanged. The percentage errors in reconstruction versus the value of M are studied.

Note that as the measurement points decreases, the spatial sampling rate drops. Eventually, distortions in reconstructed radiation patterns appear as expected.

Figure 8 depicts the L2-norm errors, which represent spatial-averaged errors in the reconstructed radiation patterns. Results show that even when M = 190 with angular resolution of $\Delta\phi_1$ =5° and $\Delta\phi_2$ =10° along the longitudinal and transverse directions, respectively, the spatial-averaged error is less than 0.8dB. This indicates that there is a potential for us to further decrease the number of input data. Our test results further show that the established relation $n = ka$ can be relaxed to

$$n = 0.023(ka)^2 - 0.0716(ka) + 6.397 \qquad (6)$$

Eq. (6) is obtained by curve-fitting the test results. It is a less stringent requirement than the established one. For example, at 12500Hz, we have ka = 19.6. Substituting ka value into Eq. (6), we obtain n = 14 rather than 20. This means that we need $J = (n + 1)^2$ = 225 expansion terms and slightly more measurement points than the expansion terms, say, M = 250, to recover all five side lobes in radiation pattern. At 16000Hz or ka = 25, we get n = 19 and J = 400, rather than n = 25 and J = 676. So M = 410 is enough to recover all seven side lobes in radiation pattern.

It must be pointed out, however, that in these cases the input data are error free whereas in reality the measured data are always contaminated by background noise. Therefore, we need to examine the robustness of HELS method with respect to erroneous input data. This is done by introducing Gaussian white noise into the field acoustic pressures generated by Eq. (5).

Figure 9 displays the comparison of reconstructed radiation patterns based on the input data that contain Gaussian-type, pseudorandom noise whose statistical profile is (μ, σ), where μ = 0 is the expected mean value, σ is the standard deviation, versus reconstructed ones with error-free input data and theoretical ones. Results show that with σ = 5% Gaussian noise, the reconstructed side lobes of radiation pattern at 6286Hz are still fairly close to that of the theoretical ones; when the measurement noise increases to σ = 10%, the basic radiation pattern is preserved but distortions are observed, which are reflected in sharpening of the main lobe and splitting of side lobes. It is noted that the radiation patterns in Figure 9 are expressed in a linear scale. If dB scale is adopted, the distortions might not seem as significant because the major distortion occurs at the main lobe and a logarithmic scale has less effect on a large value than a small value.

It is important to point out the significance of the expansion index n, which controls the details of an expansion solution. Figure 10 illustrates how the value of n can affect the reconstructed result. In this case, there are five side lobes in the radiation pattern at f = 12532Hz. When the expansion is stopped at n = 8 with a total of J = 81 expansion terms, only three of side lobes are recovered. As we increase the index to n = 12 with a total

of $J = 169$ expansion terms, all five side lobes are recovered successfully. This example shows the importance to extend an expansion solution to a high order to get all details right. The price for acquiring detailed information is that the number of measurement points must be increased substantially. Hence, in practice we must balance the accuracy with costs. In any event, this example illustrates interrelationships among the expansion index n, dimensionless frequency ka, and numbers of expansion terms J and measurement points M needed in HELS method, as well as the impact of errors imbedded in the input data on the final results.

4.3. WHAT ARE THE POTENTIAL BENEFITS OF USING HELS?

Once we have seen the results in Figures 3 to 10, it is not too difficult to get an overall picture of what potential benefits one may get by using HELS to reconstruct radiation patterns in practice. These benefits are summarized in Table 1. Basically, at low frequencies with $0 < ka \leq 1$, we can expect extremely high accuracy in reconstruction using HELS method. At mid frequencies with $1 < ka \leq 5$, the accuracy in reconstruction using HELS is still very high. At high frequencies with $5 < ka \leq 25$, we need increase the expansion index n and expansion terms in HELS formulations and measurement points in order to maintain certain level of accuracy in reconstruction and get all side lobes right. The total measurement points needed by HELS method are substantially less than those required by AES Standards however. Therefore, the HELS method enables one to get an accurate description of radiation patterns in a very cost-effective manner.

5. CONCLUSIONS

The HELS method enables one to reconstruct radiation patterns from a non-spherical source both accurately and effectively. The errors in the input data will have some effect but not substantial. In other words, HELS is quite robust. This is because the results have been regularized and errors have been minimized by the least squares method. The most significant result of this study is that HELS can produce accurate results with much fewer measurement points than those required by AES Standards. Therefore, it can become potentially a cost-effective method for visualizing the radiation pattern of a speaker.

M / *ka*	$M = 210$ 90% reduction	$M = 310$ 85% reduction	$M = 410$ 80% reduction
$0 < ka \le 1$	negligible error	negligible error	negligible error
$1 < ka \le 5$	maximum error < 0.1dB	maximum error < 0.1dB	maximum error ≈ 0.0dB
$5 < ka \le 25$	maximum error < 1.3dB	maximum error < 1.0dB	maximum error < 0.7dB

Table 1. Reduction of measurement number by using HELS method

6. REFERENCES

[1] Standards and information documents, *Audio Engineering Society*, INC., AES-5id –1997 (2003).

[2] F. Seidel and H. Staffeldt, "Frequency and Angular Resolution for measuring, presenting, and predicting loudspeaker polar data," *Journal of Audio Engineering Society*, Vol. 44, No. 7/8, 555 – 568 (1996).

[3] Wolff and L. Malter, "Directional radiation of sound," *Journal of the Acoustical Society of America*, 201 – 241 (1930).

[4] M. R. Bai and T. Huang, "Development of panel loudspeaker system: Design, evaluation and enhancement," *Journal of the Acoustical Society of America*, Vol. 109, No. 6, 2751 – 2761 (2001).

[5] Z. Wang and S. F. Wu, "Helmholtz Equation-Least Squares (HELS) method for reconstructing the acoustic pressure field," *Journal of the Acoustical Society of America*, Vol. 102, No. 4, 2020 – 2032 (1997).

[6] S. F. Wu, "On reconstruction of acoustic pressure fields using the Helmholtz equation least squares method," *Journal of the Acoustical Society of America*, Vol. 107, 2511 – 2522 (2000).

[7] G. Weinreich and E. B. Arnold, "Method for measuring acoustic radiation fields," *Journal of the Acoustical Society of America*, Vol. 68, 404 – 411 (1980).

[8] I. N. Vekua, "On completeness of a system of metaharmonic functions," *Dokl. Akad. Nauk SSSR*, 90 (5), 715 – 718 (1953) (in Russian).

[9] Victor Isakov and Sean F. Wu, "On theory and applications of the HELS method in inverse acoustics," *Inverse Problem*, Vol. 18, 1147 – 1159 (2002).

[10] L. L. Beranek, *Acoustics* (Acoustical Society of America, 105 – 106, 1993).

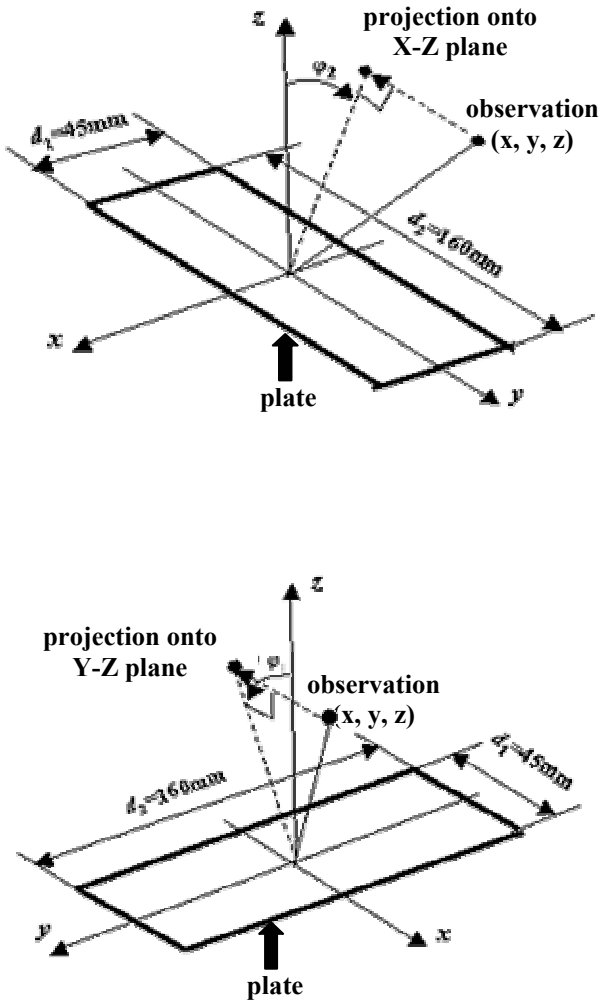

Figure 1. Schematic of a rectangular plate with a width d_1 = 45mm and length d_2 = 160mm.

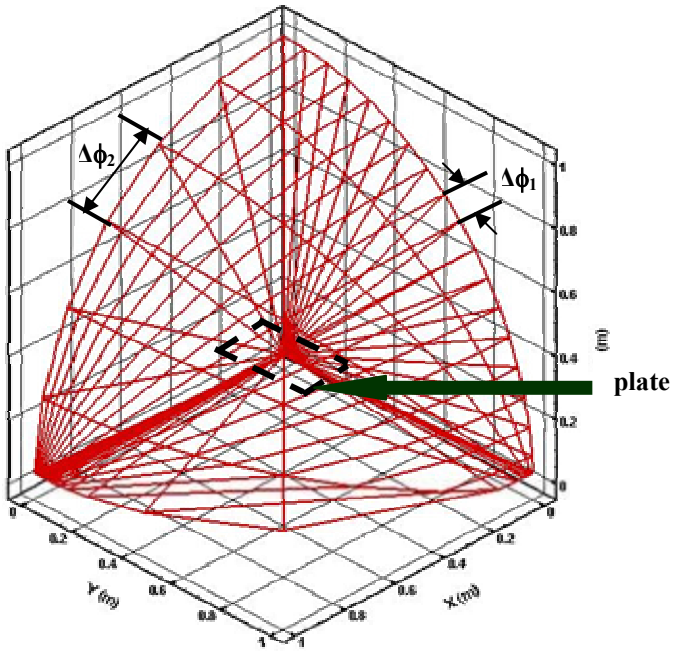

Figure 2. Schematic of the measurement points on a hemispherical surface of radius 1m. For clarity, only one quadrant of this hemispherical surface is shown.

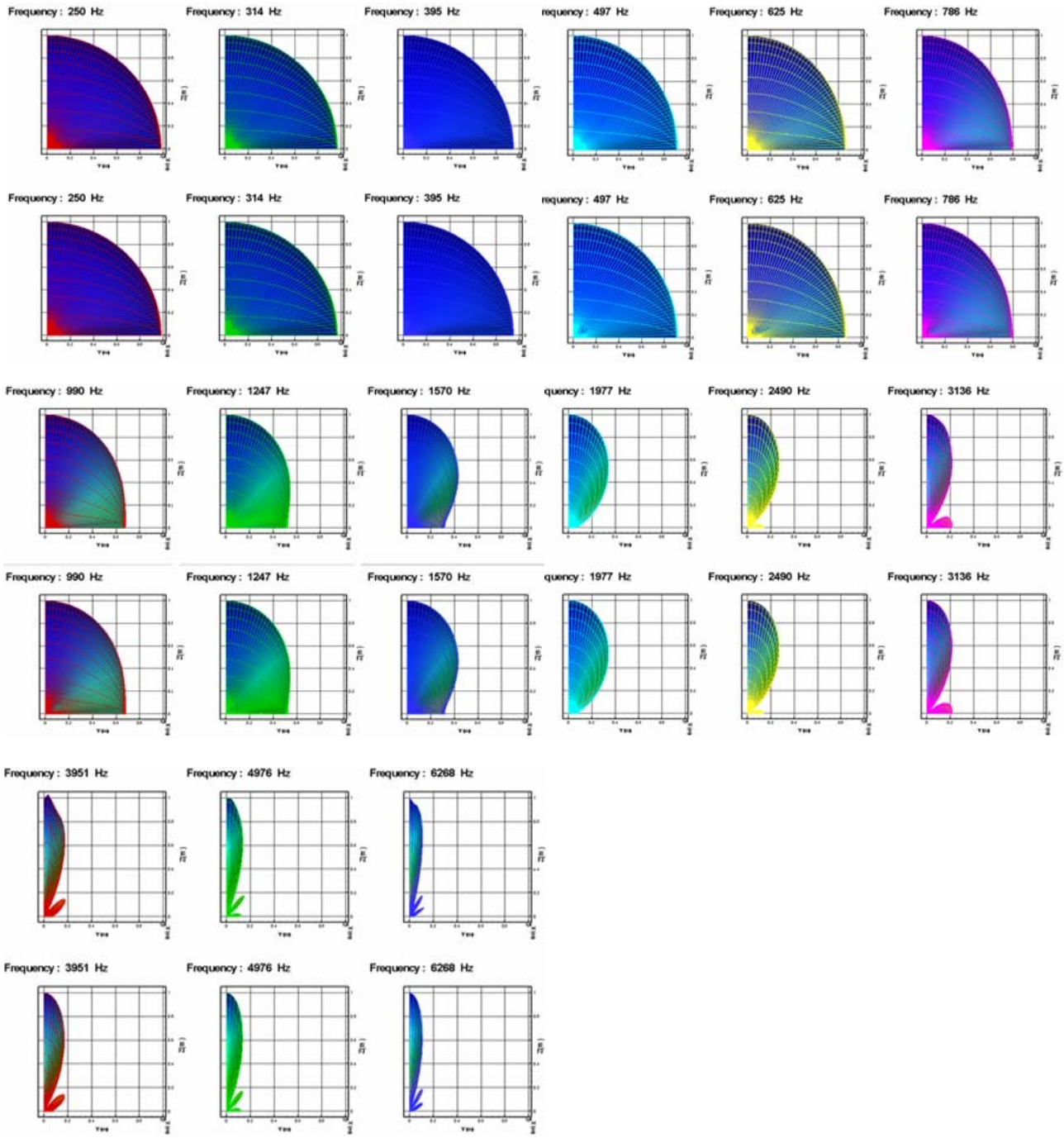

Figure 3. Comparison of the reconstructed radiation patterns and theoretical ones in a linear scale projected onto the *y-z* plane at center frequencies of 1/3-octave bands from 250 to 6268Hz (left to right). The reconstructed radiation patterns using HELS method are shown in the 1st, 3rd and 5th rows, and the theoretical radiation patterns using Eq. (5) are shown in the 2nd, 4th and 6th rows.

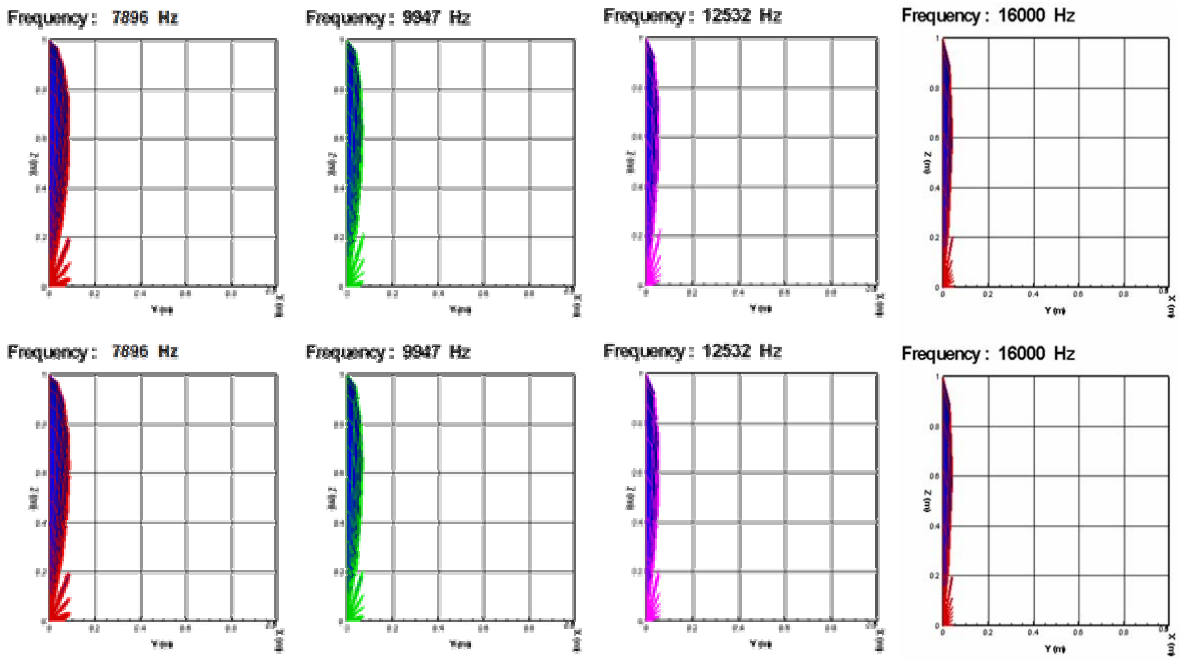

Figure 4. Comparison of the reconstructed radiation patterns and theoretical ones in a linear scale projected onto the *y-z* plane at center frequencies of 1/3-octave bands from 7896 to 16000Hz (left to right). The reconstructed radiation patterns using HELS method are shown in the 1st row, and the theoretical radiation patterns using Eq. (5) are shown in the 2nd row.

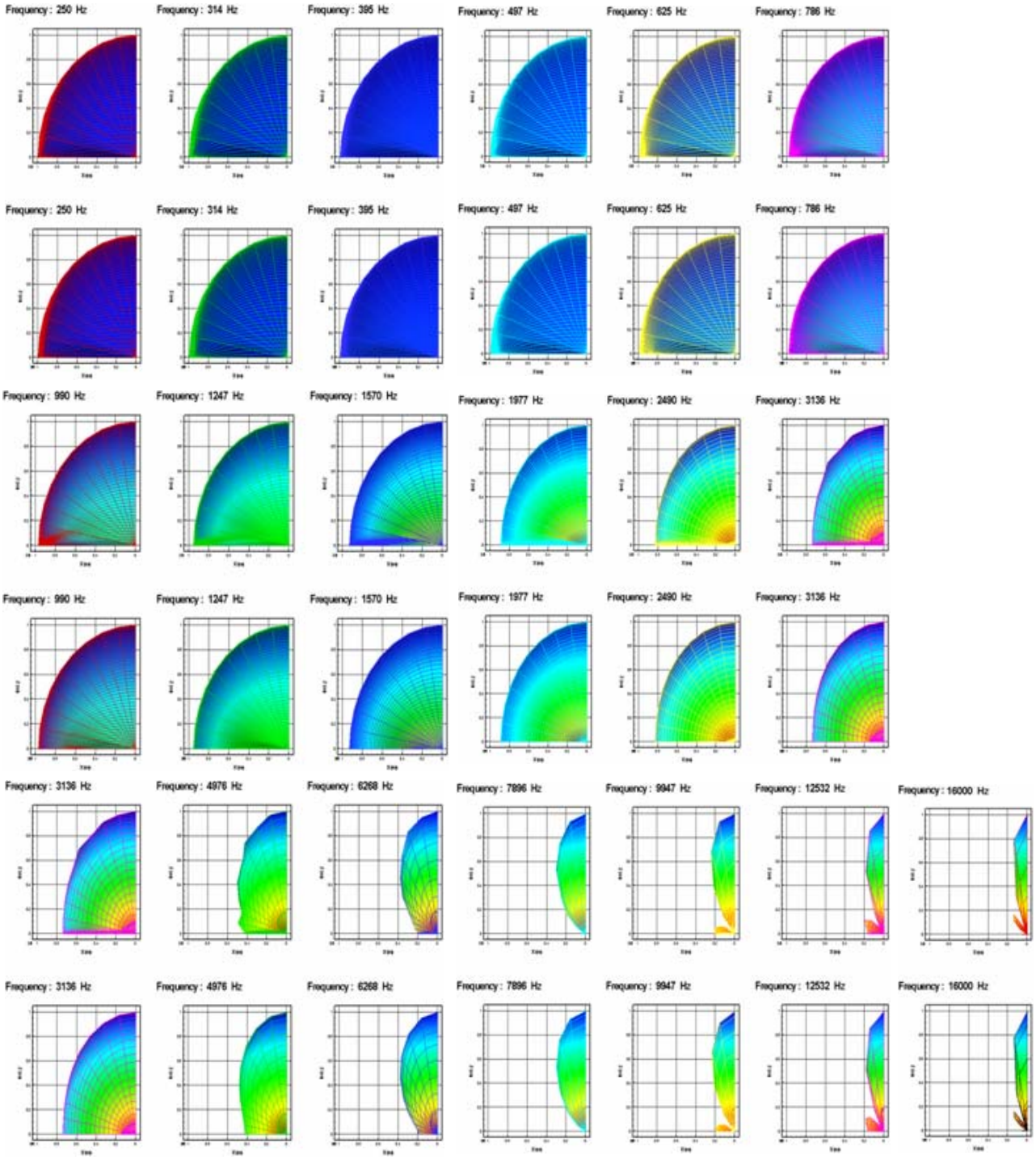

Figure 5. Comparison of the reconstructed radiation patterns and theoretical ones in a linear scale projected onto the *x-z* plane at center frequencies of 1/3-octave bands from 250 to 16000Hz (left to right). The reconstructed radiation patterns using HELS method are shown in the 1st, 3rd and 5th rows, and the theoretical radiation patterns using Eq. (5) are shown in the 2nd, 4th and 6th rows.

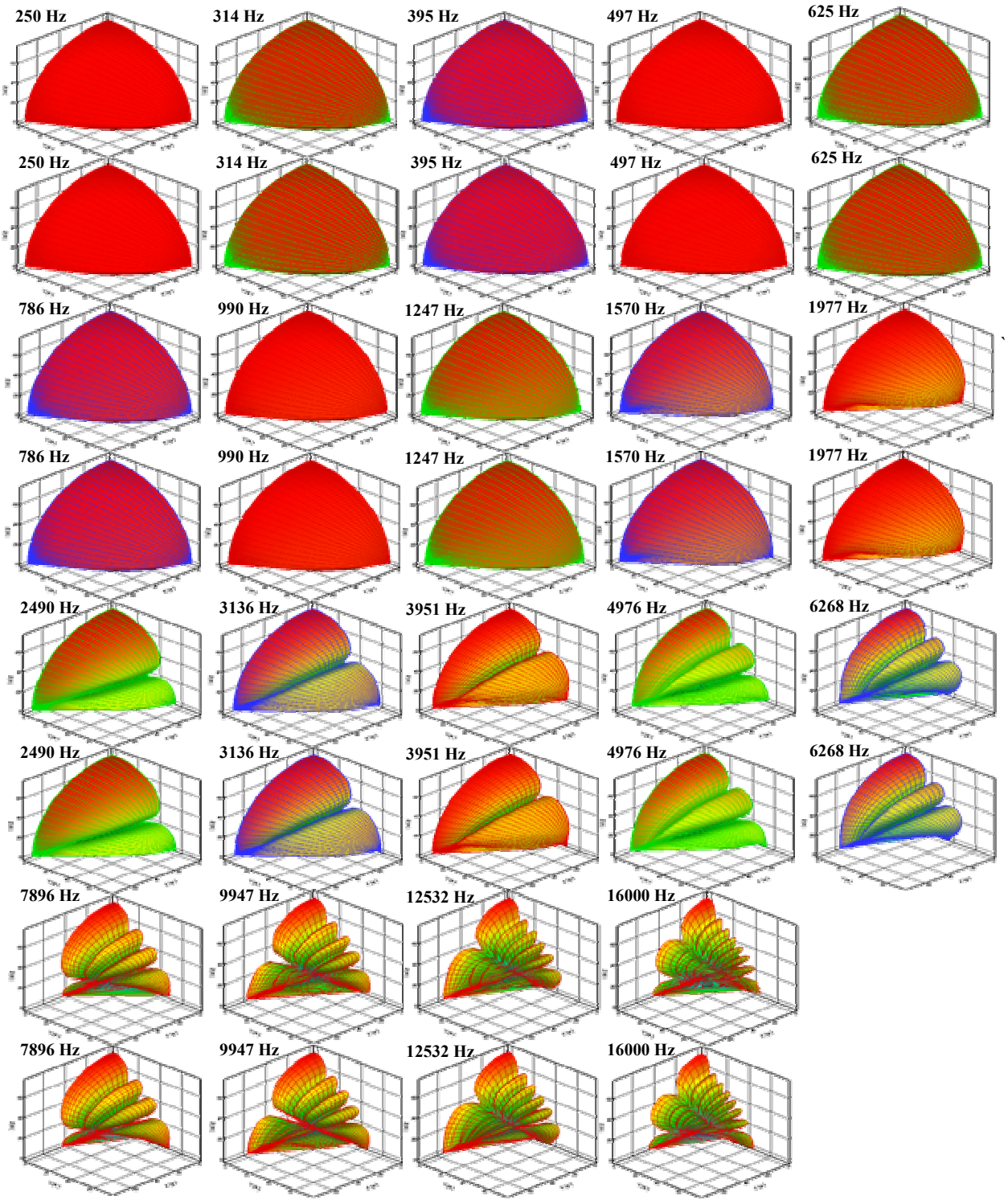

Figure 6. Comparison of the reconstructed radiation patterns and theoretical ones in 3D with dB scale at center frequencies of 1/3-octave bands from 250 to 16000Hz (left to right). The reconstructed radiation patterns using HELS method are shown in the 4 odd rows, and the theoretical radiation patterns using Eq. (5) are shown in the 4 even rows.

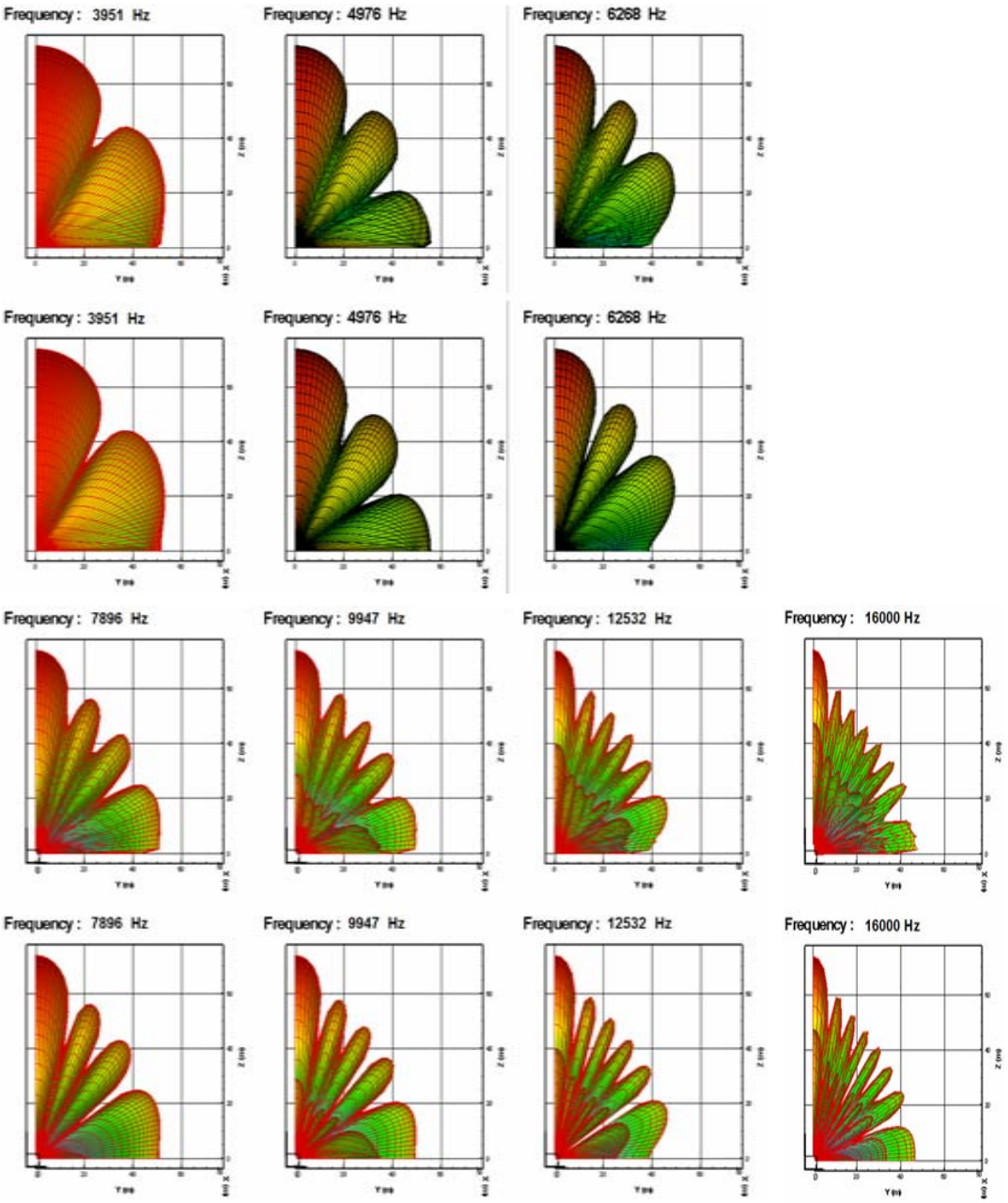

Figure 7. Comparison of the reconstructed radiation patterns and theoretical ones in 3D with dB scale but projected on the *y-z* plane at center frequencies of 1/3-octave bands from 3951 to 16000Hz (left to right). The reconstructed radiation patterns using HELS method are shown in the 1st and 3rd rows, and the theoretical radiation patterns using Eq. (5) are shown in the 2nd and 4th rows.

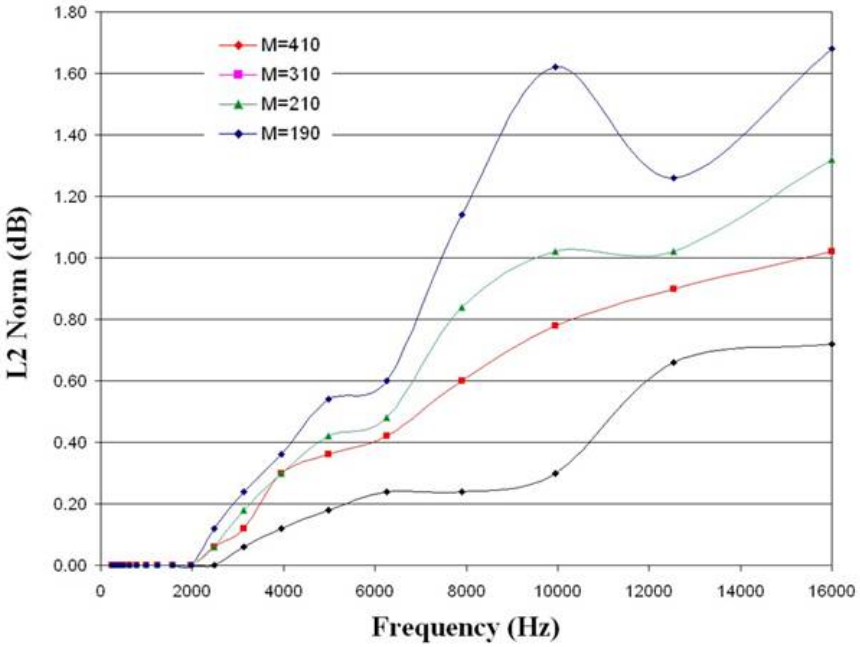

Figure 8. L2-norm errors in reconstructed radiation patterns versus frequency at different number of measurement points *M*. $\|E\|_M^N = \|P_r - P_t\|_2 / \|P_t\|_2$. P_r is the reconstructed acoustic pressure; P_t is the theoretical pressure at the same location; *M* is the measurement number; and *N* is the reconstruction number.

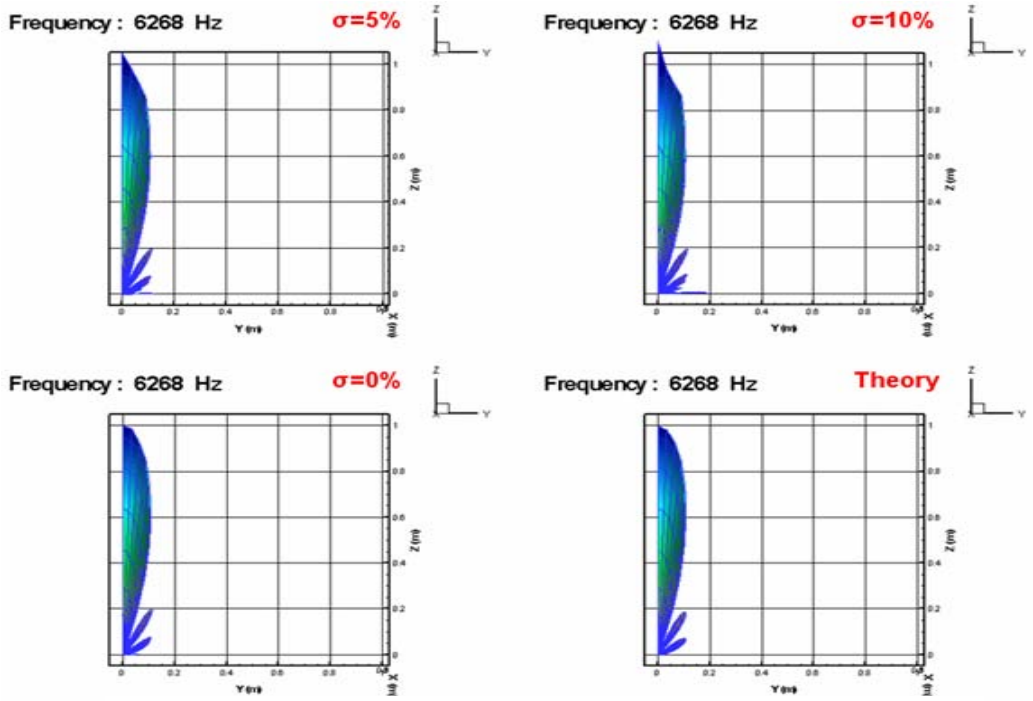

Figure 9. Comparison of reconstructed radiation patterns at 6268Hz with different amount of random errors embedded in the input data. σ is the standard deviation in Gaussian white noise.

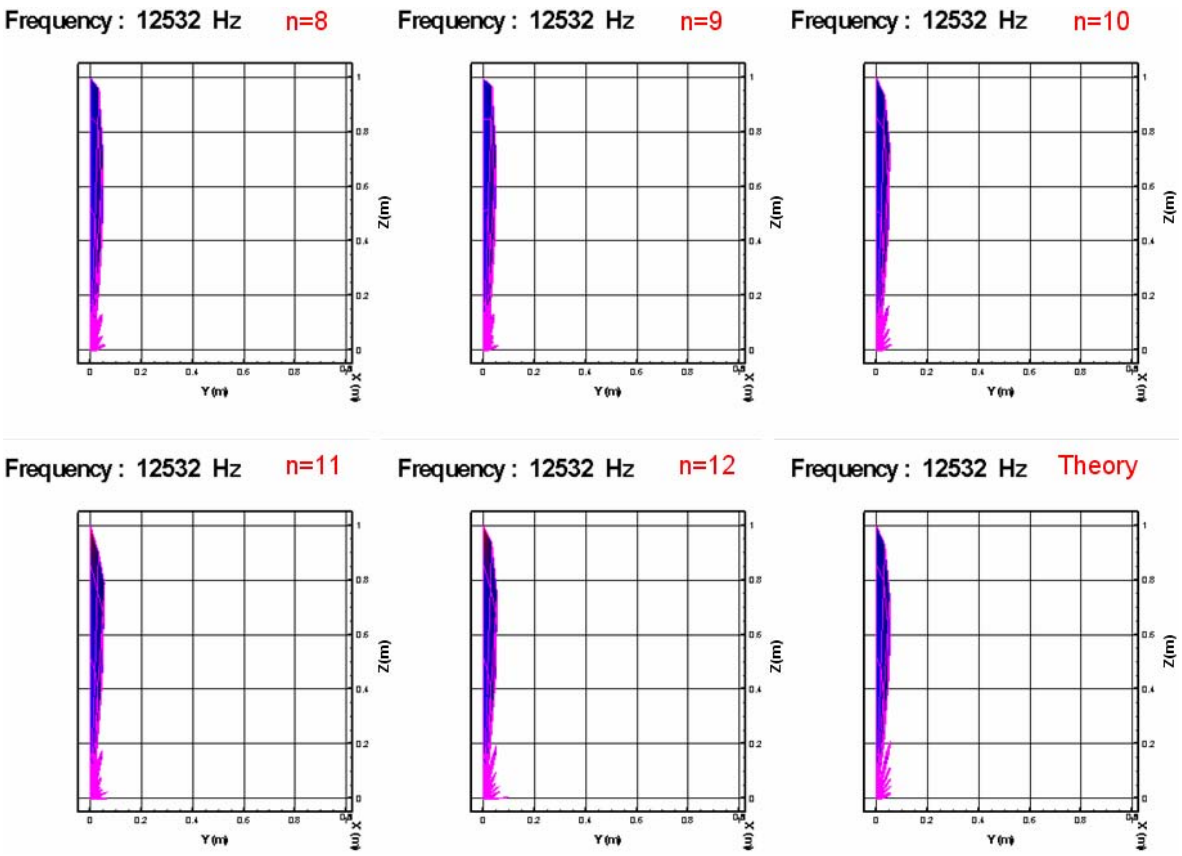

Figure 10. Impact of the index *n* in expansion on the reconstructed radiation patterns at 12532Hz. As the index *n* increases, more expansion terms are used in the HELS solutions and more side lobes can be recovered.